Applied Mathematics and Computation 222 (2013) 1–12

Contents lists available at ScienceDirect

Applied Mathematics and Computation

journal homepage: www.elsevier.com/locate/amc

Diamond in multi-layer cellular neural networks

Jung-Chao Ban [a], Chih-Hung Chang [b,*]

[a] Department of Applied Mathematics, National Dong Hwa University, Hualien 970003, Taiwan, ROC
[b] Department of Applied Mathematics, Feng Chia University, Taichung 40724, Taiwan, ROC

ARTICLE INFO

Keywords:
Multi-layer cellular neural networks
Topological entropy
Diamond
Sofic shift

ABSTRACT

This investigation considers the complexity of output spaces of multi-layer cellular neural networks. Let $\mathcal{B}$ be a set of admissible local output patterns coupled with input and let $\widetilde{\mathcal{B}}$ be the set of admissible output patterns extracting from $\mathcal{B}$. Since topological entropy is an indicator for investigating the complexity of spaces, we study the topological entropy of output spaces $\mathbf{Y_U}$ and $\mathbf{Y}$ which are induced by $\mathcal{B}$ and $\widetilde{\mathcal{B}}$, respectively. A system has a *diamond* if $h(\mathbf{Y_U}) \neq h(\mathbf{Y})$. Necessary and sufficient conditions for the existence of diamond are demonstrated separately. Furthermore, numerical experiments exhibit some novel phenomena.

1. Introduction

Cellular neural networks is a large aggregate of analogue circuit. The system presents itself as an array of identical cells which are locally coupled one another. Cellular neural networks have been widely applied in studying the signal propagation between neurons, image processing, patterns recognition, information technology and VLSI [7–9,17–19,21].

In this paper we concentrate the investigation on one dimension case. One-dimensional cellular neural networks with input is realized as

$$\frac{dx_i}{dt} = -x_i + \sum_{|k|\leqslant d} a_k y_{i+k} + \sum_{|\ell|\leqslant d} b_\ell u_{i+\ell} + z \tag{1}$$

for some $d \in \mathbb{N}$ and $i \in \mathbb{Z}$. Herein

$$y = f(x) = \frac{1}{2}(|x+1| - |x-1|) \tag{2}$$

is the output function and u_i is the *input* term. $A = [a_{-d}, \ldots, a_d]$ and $B = [b_{-d}, \ldots, b_d]$ are feedback and controlling templates, respectively, and z is the threshold. *Mosaic solutions* are crucial for studying the complexity of (1) [11,15]. A stationary solution $\bar{x} = (\bar{x}_i)$ is called *mosaic* if $|\bar{x}_i| > 1$ for all $i \in \mathbb{Z}$. Its corresponding output pattern is called *mosaic pattern*. For simplicity, we use *pattern* for the abbreviation of *mosaic pattern*. The complexity of mosaic patterns for cellular neural networks are widely studied [2,1,3,4,11,15]. Since the feedback and controlling templates are spatially invariant, the global pattern formation is thus completely determined locally. These local patterns are then called *admissible local patterns* and a collection of admissible local patterns is denoted by $\mathcal{B}$. Investigating the output space of a circuit system such as cellular neural network is then connected with symbolic spaces. Since every pattern in the output space is a bi-infinite binary string, the study of mosaic

* Corresponding author.
E-mail addresses: jcban@mail.ndhu.edu.tw (J.-C. Ban), chihhung@mail.fcu.edu.tw (C.-H. Chang).

0096-3003/$ - see front matter
http://dx.doi.org/10.1016/j.amc.2013.07.010

patterns is related to the elucidation of symbolic dynamical systems. For more details, reader is referred to [2,1,3,4,12–14,16] and the references therein.

One-dimensional multi-layer cellular neural networks are considered by coupling several layers of cellular neural networks with input. It is understood as the following form:

$$\frac{dx_i^{(n)}}{dt} = -x_i^{(n)} + \sum_{|k|\leqslant d} a_k^{(n)} y_{i+k}^{(n)} + \sum_{|\ell|\leqslant d} b_\ell^{(n)} u_{i+\ell}^{(n)} + z^{(n)}, \tag{3}$$

where $1 \leqslant n \leqslant N$ for some $N \in \mathbb{N}, i \in \mathbb{Z}$, and

$$y_i^{(n-1)} = u_i^{(n)} \quad \text{for} \quad 2 \leqslant n \leqslant N, \quad u_i^{(1)} = u_i \quad \text{is given.}$$

Since we focus on mosaic patterns, this concentrates our attention on mosaic input patterns, that is, $|u_i| = 1$ for all i. The output patterns $y^{(N)} = (y_i^{(N)})$ of the N-th layer are the only expression that can be observed since outputs $y^{(n)}$ are treated as input $u^{(n+1)}$ for $n = 1, \ldots, N-1$. Those output patterns produced by the rest $N-1$ layers never "show up" and thus these layers are called *hidden layers*. Recent research shows that hidden layers make an impact on the dynamics of the output layer such as the broken of symmetry structure of entropy diagram (cf. [2,4]). This motivates the investigation of the relation between the hidden and output layers. We will elucidate the relation based on the concept of topological entropy, it helps for the understanding of the distinction between the structure of the hidden and output layers.

The present paper devotes to build a mathematical foundation for circuit systems multi-layer cellular neural networks. Considering one-layer cellular neural networks with input, the set of admissible local output patterns coupled with input $\mathcal{B}(A, B, z)$ is determined by the templates A, B and threshold z. Let $\widetilde{\mathcal{B}}(A, B, z)$ be the set of admissible local output patterns extracting from $\mathcal{B}(A, B, z)$ and let $\mathbf{Y}$ and $\mathbf{Y_U}$ be the output spaces induced by $\widetilde{\mathcal{B}}(A, B, z)$ and $\mathcal{B}(A, B, z)$, respectively. It comes immediately $\mathbf{Y_U}$ is a factor of $\mathbf{Y}$ and therefore $h(\mathbf{Y_U}) \leqslant h(\mathbf{Y})$ [3,4,16]. $h(\mathbf{Y_U}) = h(\mathbf{Y})$ indicates the circuit system only loss a few information and $h(\mathbf{Y_U}) < h(\mathbf{Y})$ implies the losing rate of information is exponential with respect to the size of the circuit. A system satisfies $h(\mathbf{Y_U}) < h(\mathbf{Y})$ is said to *have a diamond* (cf. Definition 2.3 and Fig. 2). Although it is lack of a necessary and sufficient condition, we give necessary and sufficient conditions for the existence of diamond in one-layer cellular neural networks with input (Theorems 3.1 and 3.3).

Theorem 2.4 indicates that, for a two-layer cellular neural network, the data transmission between the first and second layers are either uncountable-to-one (in this case, there exists a diamond) or finite-to-one (no diamond is observed). Let $\mathbf{Y}_1$ and $\mathbf{Y}_2$ be the output spaces of the first and second layers, respectively. Suppose there exists a factor map ϕ, for instance, from $\mathbf{Y}_1$ to $\mathbf{Y}_2$. There are many finer structure in this system such as the following. Suppose $\mathbf{Y}_1$ and $\mathbf{Y}_2$ are both Markov systems. How to estimate the *degree* of ϕ (cf. [6])? Notable, investigating the degree of ϕ clarifies the memory of $\mathbf{Y}_1$ and $\mathbf{Y}_2$. There are many affirmative results if ϕ is finite-to-one. However, it remains an popular issue and is unsolved in general. Suppose $\mathbf{Y}_1$ and $\mathbf{Y}_2$ are both strict sofic shifts. There is still no result so far based on our knowledge.

An essential problem is the existence of the factor ϕ if we already know that a diamond is observed. Ban et al. [3] proposed a methodology to demonstrate the existence of ϕ. But a necessary and sufficient condition is still unclear.

The existence of diamond infers the existence of so-called *compensation function* (cf. [6, Section 3.3]). The compensation function helps for the investigation of the finest structure between $\mathbf{Y}_1$ and $\mathbf{Y}_2$. More specifically, if there exists a compensation function ξ, then ϕ would behave like a finite-to-one factor under ξ's effect. Recently, Yayama [20, Theorem 3.2] investigated the statistical mechanism of the compensation function (cf. [20] and references 91–93 and 97 in [6]). The qualitative behavior of the compensation function remains unclear in most cases. We remark that the investigation of the compensation function is equivalent to elucidate diamonds between two spaces. Last but not least, neither the correspondence between diamonds and compensation functions nor the correspondence between diamonds and infinite-to-one factors are theoretically demonstrated. However, investigating these issues help for the understanding of the inner structure of these systems. In this paper we propose some results, theoretically and numerically, to answer above questions.

Except for the criterion of the existence of diamond, we also obtain some interesting consequences via numerical experiments. Many numerical results show that there is a symmetrical structure in topological entropy of one-layer cellular neural networks without input and the symmetry is broken when input terms are considered (cf. Fig. 4). Propositions 2.1 and 2.2 demonstrate the symmetry comes from the topological conjugacy of two systems. Moreover, numerical experiments show us many novel results (Facts 1–5). For example, we find a set of parameters that has diamonds for any set of input patterns. We have two conjectures about these phenomena and are still working on them.

The rest of this elucidation is organized as follows. The upcoming section gives a brief introduction for the definitions and results of one-layer cellular neural networks and symbolic dynamical systems. Section 3 investigates the necessary and sufficient conditions for the existence of diamond. Some numerical experiments are proposed. Proof of our results are postponed until Section 4. The last section relates conclusion and discussion.

2. Preliminary

For reader's convenience, we recall some definitions and known results first. To ease the discussion, suppose $d = 1$ and $a_{-1} = b_{-1} = 0$. That is, every cell only receive signals from the nearest cell on its righthand side. (1) is then reduced as the form

$$\frac{dx_i}{dt} = -x_i + ay_i + a_1 y_{i+1} + bu_i + b_1 u_{i+1} + z. \tag{4}$$

Considering the set of mosaic solutions, we denote patterns "-1" and "1" by symbols "$-$" and "$+$", respectively. It is seen that the necessary and sufficient condition for "$+$" at cell C_i, i.e., $x_i > 1$, is

$$a + z - 1 > -a_1 \bar{y}_{i+1} - (bu_i + b_1 u_{i+1}). \tag{5}$$

Similarly, the necessary and sufficient condition for "$-$" at cell C_i is

$$a - z - 1 > a_1 \bar{y}_{i+1} + (bu_i + b_1 u_{i+1}). \tag{6}$$

With abuse of the notation we denote $\bar{y} = (\bar{y}_i)$ by $y = (y_i)$. Moreover, representing the local output patterns $y_0 y_1$ coupled with input $u_0 u_1$ as

$$\begin{matrix} y_0 y_1 \\ u_0 u_1 \end{matrix} := y_0 y_1 \diamondsuit u_0 u_1 \quad \text{for simplicity.}$$

Let $\mathcal{B}(A,B,z) \subseteq \{-,+\}^{\mathbb{Z}_{2\times 2}}$ be the set of admissible local patterns with respect to A, B and z. Denote the parameter space by $\mathcal{P} = \{(A,B,z)\}$. Every $\mathcal{B}(A,B,z)$ is related to a partition of $\mathcal{P}$. Reader is referred to [4,10].

Since we concern mosaic output patterns, it is natural to request the input term $u = (u_i)$ being mosaic. That is, $u_i \in \{-,+\}$ for $i \in \mathbb{Z}$. Suppose parameters a_1, b, b_1 are fixed, (5) and (6) partition (a,z)-space into 81 subregions. Numbering these subregions by a pair $[m,n]$ for $0 \leqslant m, n \leqslant 8$, where m and n stands for the number of inequalities in (5) and (6) the parameters a and z satisfy. More specific,

$$\begin{aligned} m &= \#\{y \in \{-,+\} : +y \diamondsuit u_0 u_1 \in \mathcal{B}(A,B,z) \text{ for some } y, u_0, u_1 \in \{-,+\}\}, \\ n &= \#\{y \in \{-,+\} : -y \diamondsuit u_0 u_1 \in \mathcal{B}(A,B,z) \text{ for some } y, u_0, u_1 \in \{-,+\}\}. \end{aligned}$$

Topological entropy is frequently used to elucidate the complexity of output space derived by $\mathcal{B}(A,B,z)$. Given $\mathcal{B} \subseteq \{-,+\}^{\mathbb{Z}_{2\times 2}}$, set $\Sigma_n(\mathcal{B}) \subseteq \{-,+\}^{\mathbb{Z}_{n\times 2}}$ by

$$\Sigma_n(\mathcal{B}) := \{y_1 \ldots y_n \diamondsuit u_1 \ldots u_n : y_i y_{i+1} \diamondsuit u_i u_{i+1} \in \mathcal{B} \text{ for all } i\}.$$

The *topological entropy* $h(\mathcal{B})$ is defined by

$$h(\mathcal{B}) = \lim_{n\to\infty} \frac{\log \#\Sigma_n(\mathcal{B})}{n}. \tag{7}$$

The existence of the limit comes from the submultiplicativity of $\#\Sigma_n(\mathcal{B})$ (cf. [16]), where $\#E$ indicates the cardinality of E. Define the ordering matrix of $\{-,+\}^{\mathbb{Z}_{2\times 2}}$ by

$$\mathbb{X} = \left(\begin{array}{cc|cc} \boxed{\begin{smallmatrix} -- \\ -- \end{smallmatrix}} & \boxed{\begin{smallmatrix} -- \\ -+ \end{smallmatrix}} & \boxed{\begin{smallmatrix} -+ \\ -- \end{smallmatrix}} & \boxed{\begin{smallmatrix} -+ \\ -+ \end{smallmatrix}} \\ \boxed{\begin{smallmatrix} -- \\ +- \end{smallmatrix}} & \boxed{\begin{smallmatrix} -- \\ ++ \end{smallmatrix}} & \boxed{\begin{smallmatrix} -+ \\ +- \end{smallmatrix}} & \boxed{\begin{smallmatrix} -+ \\ ++ \end{smallmatrix}} \\ \hline \boxed{\begin{smallmatrix} +- \\ -- \end{smallmatrix}} & \boxed{\begin{smallmatrix} +- \\ -+ \end{smallmatrix}} & \boxed{\begin{smallmatrix} ++ \\ -- \end{smallmatrix}} & \boxed{\begin{smallmatrix} ++ \\ -+ \end{smallmatrix}} \\ \boxed{\begin{smallmatrix} +- \\ +- \end{smallmatrix}} & \boxed{\begin{smallmatrix} +- \\ ++ \end{smallmatrix}} & \boxed{\begin{smallmatrix} ++ \\ +- \end{smallmatrix}} & \boxed{\begin{smallmatrix} ++ \\ ++ \end{smallmatrix}} \end{array}\right)$$

Since the ordering matrix indicates how those patterns of given length are generated by admissible local patterns, it is used for the examination of the topological entropy. Reader is referred to [4,5] for more details. Every $\mathcal{B}$ corresponds to an ordering matrix $\mathbb{X}(\mathcal{B})$. For those $y_0 y_1 \diamondsuit u_0 u_1 \notin \mathcal{B}$, we substitute them as $\emptyset$. The transition matrix $\mathbf{T}(\mathcal{B})$ of $\mathcal{B}$ is a $0-1$ matrix defined by

$$t_{ij} = \begin{cases} 1, & x_{ij} \neq \emptyset; \\ 0, & x_{ij} = \emptyset. \end{cases}$$

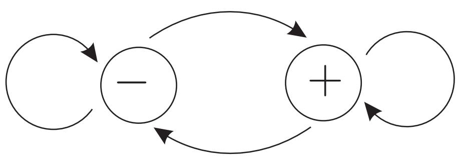

Fig. 1. Graph representation of all admissible local patterns for one- layer cellular neural networks without input.

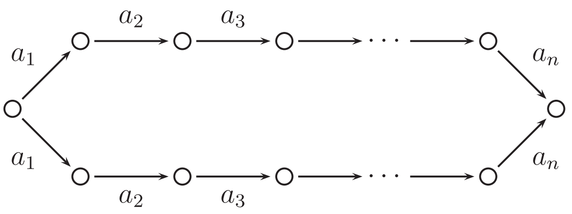

Fig. 2. Graph representation of diamond.

where $\mathbf{T}(\mathcal{B}) = (t_{ij})_{1\leqslant i,j\leqslant 4}$ and $\mathbb{X}(\mathcal{B}) = (x_{ij})_{1\leqslant i,j\leqslant 4}$. The transition matrix plays a key role for the calculation of topological entropy of the output space of $\mathcal{B}$ (cf. [4,11,12]). Positive topological entropy demonstrates $\#\Sigma_n(\mathcal{B})$ increases exponentially and $h(\mathcal{B}) = 0$ indicates polynomial growth rate of $\#\Sigma_n(\mathcal{B})$.

Suppose $b = b_1 = 0$, i.e., considering cellular neural networks without input. A necessary and sufficient condition for $h(\mathcal{B}(A,z)) > 0$ is given.

Proposition 2.1. *Suppose that $b = b_1 = 0$. Given $A = [a, a_1]$ and z, denote by $\mathcal{B}(A,z)$ the set of admissible local patterns induced by A and z. Let $0 \leqslant m, n \leqslant 2$ be the number of local patterns with $y_0 = +$ and $y_0 = -$, respectively. Then*

$$h(\mathcal{B}(A,z)) > 0 \quad \Longleftrightarrow \quad \begin{cases} m+n = 4, & a_1 > 0; \\ m+n \geqslant 3, & a_1 < 0. \end{cases}$$

An intuitive explanation for Proposition 2.1 is the graph representation of the admissible local patterns (cf. Fig. 1). m and n assert how many edges are concluded in the graph representation of $\mathcal{B}(A,z)$. An output space $\mathbf{X}$ that has a graph representation is called a one-step shift of finite type (SFT).

Let $\mathbf{X}_1, \mathbf{X}_2$ be two shift spaces with shift maps σ_1, σ_2, where $\sigma_i : \mathbf{X}_i \to \mathbf{X}_i$ is defined by $(\sigma_i(x))_k = x_{k+1}$ for $k \in \mathbb{Z}, i = 1,2$. A map $\phi : \mathbf{X}_1 \to \mathbf{X}_2$ satisfies $\sigma_2 \circ \phi = \phi \circ \sigma_1$ is called *factor map* if ϕ is onto. We say that $\mathbf{X}_1$ is topological conjugate to $\mathbf{X}_2$ if and only if there exists a one-to-ont factor map from $\mathbf{X}_1$ to $\mathbf{X}_2$.

Suppose the parameters in (4) are determined except a and z. There is a one-to-one correspondence between the sets of admissible local patterns $\{\mathcal{B}(A,B,z)\}$ and subregions $\{[m,n]\}_{0\leqslant m,n\leqslant 8}$. For the sake of clarity we denote $\mathcal{B}(A,B,z)$ by $\mathcal{B}([n,m])$. Let

$$\mathbf{X}_{\mathcal{B}([n,m])} = \{(y_i) \in \{-,+\}^{\mathbb{Z}} : \exists (u_i) \in \{-,+\}^{\mathbb{Z}} \text{ such that } \quad y_i y_{i+1} \Diamond u_i u_{i+1} \in \mathcal{B}([n,m]) \text{ for } i \in \mathbb{Z}\} \tag{8}$$

be the output space induced by $\mathcal{B}([n,m])$.

Proposition 2.2. *Suppose that $a_1, b, b_1 \in \mathbb{R}$ are fixed. For $0 \leqslant m, n \leqslant 8, \mathbf{X}_{\mathcal{B}([m,n])}$ is topological conjugate to $\mathbf{X}_{\mathcal{B}([n,m])}$.*

Proposition 2.2 explains why the topological entropy diagram is symmetric when there is no external input patterns added. See the top diagram in Fig. 3. We postpone the proof to the last section.

Suppose $\mathbf{X}_1, \mathbf{X}_2$ are two shift spaces and $\phi : \mathbf{X}_1 \to \mathbf{X}_2$ is a one-block factor map, that is, $(\phi(x))_n = \phi(x_n)$ for $x \in \mathbf{X}_1, n \in \mathbb{Z}$. We introduce a so-called *diamond* that measures the loss of information caused by the factor map ϕ.

Definition 2.3. If there exist $i_1 \ldots i_k \neq j_1 \ldots j_k \in \Sigma_n(\mathbf{X}_1)$ with $i_1 = j_1, i_k = j_k$ and $\phi(i_1 \ldots i_k) = \phi(j_1 \ldots j_k)$, where $\Sigma_n(\mathbf{X})$ consists of all admissible words in $\mathbf{X}$ of length n. Then we say ϕ has a *diamond*.

Fig. 2 illustrates graph representation of a diamond. The following theorem indicates a necessary and sufficient condition for examining whether a factor map has a diamond.

Theorem 2.4 [12, Theorem 4.1.7]. *Suppose $\phi : \mathbf{X}_1 \to \mathbf{X}_2$ is a one-block factor map between irreducible shifts of finite type and $h(\mathbf{X}_1) > 0$. Then either*

(1) ϕ is uniformly bounded-to-one,
(2) ϕ has no diamond and
(3) $h(\mathbf{X}_1) = h(\mathbf{X}_2)$

or

(1) ϕ is uncountable-to-one on some point,
(2) ϕ has a diamond and
(3) $h(\mathbf{X}_1) > h(\mathbf{X}_2)$.

Theorem 2.4 demonstrates that the investigation of existence of diamond between $\mathbf{X}_1$ and $\mathbf{X}_2$ is equivalent to investigating whether $h(\mathbf{X}_1) = h(\mathbf{X}_2)$ or not. The computation of topological entropy of one-layer cellular neural networks with input is essential for the computation of topological entropy of multi-layer cases. We illustrate a brief review for the computation of topological entropy of one-layer cellular neural networks with input. Reader is referred to [2,1,4,12] and the references therein for more details.

An output space $\mathbf{Y}$ is called *sofic shift* if $\mathbf{Y}$ has a labeled graph representation.[1] Suppose $\mathbf{Y_U}$ is an output space of some one-layer neural network with input. Then $\mathbf{Y_U}$ is a sofic shift [4]. Denote by s_1, s_2, s_3, s_4 the output patterns $--, -+, +-, ++$ respectively. Suppose $\mathcal{B}(A, B, z)$ is determined. We define the symbolic transition matrix $\widetilde{\mathbf{T}}(\mathcal{B}(A, B, z)) = (\widetilde{t}_{ij})$ by

$$\widetilde{t}_{ij} = \begin{cases} s_\ell, & x_{ij} \neq \emptyset \text{ and } s_\ell \text{ is the top pattern of } x_{ij}; \\ \emptyset, & \text{otherwise.} \end{cases}$$

where $\mathbb{X}(\mathcal{B}(A, B, z)) = (x_{ij})$ is the ordering matrix derived from $\mathcal{B}(A, B, z)$. The incidence matrix $\mathbf{T}(\mathcal{B}(A, B, z)) = (t_{ij})$ of $\widetilde{\mathbf{T}}(\mathcal{B}(A, B, z))$ is defined by

$$t_{ij} = \begin{cases} 1, & \widetilde{t}_{ij} \neq \emptyset; \\ 0, & \text{otherwise.} \end{cases}$$

A labeled graph is called *right-resolving* if all edges start from the same vertex carrying different symbols. Similarly, the symbolic transition matrix $\widetilde{\mathbf{T}}(\mathcal{B}(A, B, z))$ is right-resolving if it has right-resolving labeled graph representation. In other words, $\widetilde{\mathbf{T}}(\mathcal{B}(A, B, z))$ is right-resolving if for each row every symbol occurs at most once. The topological entropy of $\mathbf{Y_U}$ is $h(\mathbf{Y_U}) = \log \rho(\mathbf{T})$ if $\widetilde{\mathbf{T}}$ is right-resolving, where $\rho(\mathbf{T})$ is the spectral radius of $\mathbf{T}$. If $\widetilde{\mathbf{T}}$ is not right-resolving, then applying the so-called *subset construction method*[2] on $\widetilde{\mathbf{T}}$ is necessary for the computation of the topological entropy of $\mathbf{Y_U}$. We refer reader to [16].

3. Diamond: uncountable-to-one factor

3.1. Necessary and sufficient conditions for diamond

Suppose A, B and z are given. Let $\mathcal{B}(A, B, z)$ be the set of admissible local patterns. Define $\widetilde{\mathcal{B}}(A, B, z)$ the set of admissible local output patterns by

$$\widetilde{\mathcal{B}}(A, B, z) := \{y_0 y_1 \in \{-, +\}^{\mathbb{Z}_{2\times 1}} : \exists\ u_0 u_1 \in \{-, +\}^{\mathbb{Z}_{2\times 1}} \quad \text{such that} \quad y_0 y_1 \diamondsuit u_0 u_1 \in \mathcal{B}(A, B, z)\}.$$

For each pattern $y_0 y_1 \in \widetilde{\mathcal{B}}(A, B, z)$, denote by $\mathcal{I}(y_0 y_1)$ the collection of input patterns of $y_0 y_1$. That is,

$$\mathcal{I}(y_0 y_1) = \{u_0 u_1 \in \{-, +\}^{\mathbb{Z}_{2\times 1}} : y_0 y_1 \diamondsuit u_0 u_1 \in \mathcal{B}(A, B, z)\}.$$

Define the output space $\mathbf{Y_U}$ and the projection space $\mathbf{Y}$ by

$$\mathbf{Y_U} = \{(y_i)_{i\in\mathbb{Z}} : \exists\ u_i u_{i+1} \in \{-, +\}^{\mathbb{Z}_{2\times 1}} \quad \text{such that} \quad y_i y_{i+1} \diamondsuit u_i u_{i+1} \in \mathcal{B}(A, B, z) \text{ for } i \in \mathbb{Z}\},$$
$$\mathbf{Y} = \{(y_i)_{i\in\mathbb{Z}} : y_i y_{i+1} \in \widetilde{\mathcal{B}}(A, B, z) \text{ for } i \in \mathbb{Z}\}.$$

It is clear that $\mathbf{Y_U} \subseteq \mathbf{Y}$.

Theorem 3.1. *If $\#\mathcal{I}(y_0 y_1) \geqslant 2$ for each $y_0 y_1 \in \widetilde{\mathcal{B}}(A, B, z)$, then there is no diamond in $\mathbf{Y_U}$. In this case, $h(\mathbf{Y_U}) = h(\mathbf{Y})$.*

Theorem 3.1 indicates the necessary condition for diamond is

$$\exists\ y_0 y_1 \in \widetilde{\mathcal{B}}(A, B, z) \quad \text{such that} \quad \#\mathcal{I}(y_0 y_1) = 1. \qquad (D)$$

Nevertheless, (D) is not a sufficient condition for seeking diamond.

Example 3.2. Suppose that A, B and z satisfy

$$a_1 > b > -b_1 > 0, \quad a_1 > b - b_1$$

and $m = n = 5$. That is, the set of admissible local patterns $\widetilde{\mathcal{B}}(A, B, z)$ consists of

$$--\diamondsuit--, \quad --\diamondsuit-+, \quad --\diamondsuit+-, \quad --\diamondsuit++, \quad -+\diamondsuit-+,$$

$$+-\diamondsuit+-, \quad ++\diamondsuit--, \quad ++\diamondsuit-+, \quad ++\diamondsuit+-, \quad ++\diamondsuit++.$$

[1] A labeled graph is a directed graph G paired with a set of labeling $\mathcal{L}$ assigned on the edges. $\mathbf{Y}$ has a labeled graph representation means, for each $y \in \mathbf{Y}$, there is an infinite path in G whose label is y. Fig. 3 is a labeled graph representation for cellular neural networks.

[2] Roughly speaking, yielding the subset construction method creates a right-resolving labeled graph which has more vertices than the original one, and yet these two graphs present the same space. In other words, the cost of making a right-resolving graph is to increase the "size" of the graph.

Let s_1, s_2, s_3, s_4 denote the output patterns $--, --, +-, ++$ respectively. The symbolic transition matrix

$$\mathbf{T} = \begin{pmatrix} s_1 & s_1 & \varnothing & s_2 \\ s_1 & s_1 & \varnothing & \varnothing \\ \varnothing & \varnothing & s_4 & s_4 \\ s_3 & \varnothing & s_4 & s_4 \end{pmatrix}$$

and the projection space $\mathbf{Y}$ is a full shift with topological entropy $h(\mathbf{Y}) = \log 2$. Since the labeled graph representation of $\mathbf{T}$ is not right-resolving, applying subset construction is necessary for the computation of topological entropy of $\mathbf{Y_U}$. It can be verified that the symbolic transition matrix derived by applying subset construction on $\mathbf{T}$ is

$$\mathbf{H} = \begin{pmatrix} \varnothing & \varnothing & \varnothing & s_2 & s_1 & \varnothing \\ \varnothing & \varnothing & \varnothing & \varnothing & s_1 & \varnothing \\ \varnothing & \varnothing & \varnothing & \varnothing & \varnothing & s_4 \\ s_3 & \varnothing & \varnothing & \varnothing & \varnothing & s_4 \\ \varnothing & \varnothing & \varnothing & s_2 & s_1 & \varnothing \\ s_3 & \varnothing & \varnothing & \varnothing & \varnothing & s_4 \end{pmatrix}$$

and therefore $h(\mathbf{Y_U}) = \log 2$. That means there is no diamond in this case.

Suppose $\mathcal{G} = (G, \mathcal{L})$ is the labeled graph derived from a two-layer cellular neural network. A *graph diamond* for $\mathcal{L}$ is a pair of distinct paths in G having the same $\mathcal{L}$-label, the same initial state, and the same terminal state. Moreover, G is called *essential* if for every vertex v there are edges e_1, e_2 such that $i(e_1) = v$ and $t(e_2) = v$, where $i(e)$ and $t(e)$ indicate the initial and terminal states of an edge e.

It is well-known that if G is essential, then $\phi : \mathbf{Y} \to \mathbf{Y_U}$ has a diamond if and only if $\mathcal{L}$ has a graph diamond. Moreover, the transition matrix $\mathbf{T}$ gives a sufficient criterion for the existence of diamond.

Theorem 3.3. *If ϕ has a diamond, then there exists $n \in \mathbb{N}$ such that $\mathbf{T}^n(k,k) > 2$ for some k.*

We point out that Theorem 3.3 can not be enhanced to be a necessary and sufficient condition for the existence of diamond. An example is illustrated as follows.

Example 3.4. Suppose $\mathcal{A} = \{0, 1\}$. Let $\mathbf{X} \subset \mathcal{A}^{\mathbb{Z}}$ be the set of binary sequences so that between any two 1's there are even number of 0's. A labeled graph representation $\mathcal{G}$ for $\mathbf{X}$ as follows.

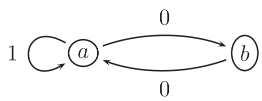

The transition matrix for $\mathbf{X}$ is

$$\mathbf{T} = \begin{pmatrix} 1 & 1 \\ 1 & 0 \end{pmatrix}.$$

It is seen that $\mathbf{T}^3(1,1) = 3$. Nevertheless, $\mathcal{G}$ has no graph diamond since it is right-resolving.

3.2. Numerical results

Aside from theoretical investigation for topological entropy and the existence of diamond, there are some interesting numerical results. First we consider one-layer cellular neural networks with input

$$\frac{dx_i}{dt} = -x_i + ay_i + a_1 y_{i+1} + bu_i + b_1 u_{i+1} + z.$$

Let $\mathbf{Y_U}$ and $\mathbf{Y}$ be the output and projection spaces, respectively.

Question 1. Under which partition of the parameter space can we see diamonds, that is, $h(\mathbf{Y_U}) < h(\mathbf{Y})$? Suppose $h(\mathbf{Y_U}) < h(\mathbf{Y})$, is there any relation between feedback and controlling templates?

We do not have a complete theoretical result for Question 1 but some partial results from numerical experiments. Table 1 lists the number of output space whose topological entropy $h(\mathbf{Y_U}) > 0$ and the ratio of subregions that have diamond in every partition. Some novel phenomena cause our interest.

Fact 1. Diamond occurs if $|b_1| > |a_1|$.

Table 1
The ratio of diamond. $1, 2$, and 3 stands for $|a_1|, |b|$, and $|b_1|$, respectively. The first column represents the sign of a_1, b and b_1, and $m_1 > m_2 > m_3$ is the magnitude of $|a_1|, |b|, |b_1|$ in descending order. Numbers before and in the parentheses is the ratio of diamond and the number of output spaces $\mathbf{Y_U}$ with nonzero topological entropies.

	$1>2>3$	$1>3>2$	$2>1>3$	$2>3>1$	$3>1>2$	$3>2>1$
$(a)\ m_1 > m_2 + m_3$						
$(+,+,+)$	0.313(16)	0.313(16)	0.182(33)	0.293(41)	0.250(36)	0.310(42)
$(+,+,-)$	0.000(16)	0.000(16)	0.000(36)	0.250(48)	0.286(35)	0.444(45)
$(+,-,+)$	0.000(16)	0.000(16)	0.000(36)	0.250(48)	0.286(35)	0.444(45)
$(+,-,-)$	0.313(16)	0.313(16)	0.182(33)	0.293(41)	0.250(36)	0.310(42)
$(-,+,+)$	0.000(44)	0.000(44)	0.000(52)	0.083(48)	0.113(53)	0.275(51)
$(-,+,-)$	0.313(48)	0.313(48)	0.182(55)	0.364(55)	0.250(60)	0.417(60)
$(-,-,+)$	0.313(48)	0.313(48)	0.182(55)	0.364(55)	0.250(60)	0.417(60)
$(-,-,-)$	0.000(44)	0.000(44)	0.000(52)	0.083(48)	0.113(53)	0.275(51)
$(b)\ m_1 < m_2 + m_3$						
$(+,+,+)$	0.480(25)	0.480(25)	0.394(33)	0.463(41)	0.444(36)	0.476(42)
$(+,+,-)$	0.000(25)	0.000(25)	0.000(36)	0.250(48)	0.286(35)	0.444(45)
$(+,-,+)$	0.000(25)	0.000(25)	0.000(36)	0.250(48)	0.286(35)	0.444(45)
$(+,-,-)$	0.480(25)	0.480(25)	0.394(33)	0.463(41)	0.444(36)	0.476(42)
$(-,+,+)$	0.000(49)	0.000(47)	0.000(52)	0.083(48)	0.082(49)	0.245(49)
$(-,+,-)$	0.509(55)	0.509(55)	0.418(55)	0.564(55)	0.467(60)	0.600(60)
$(-,-,+)$	0.509(55)	0.509(55)	0.418(55)	0.564(55)	0.467(60)	0.600(60)
$(-,-,-)$	0.000(49)	0.000(47)	0.000(52)	0.083(48)	0.082(49)	0.245(49)

Fact 2. Suppose $|a_1| > |b_1|$. Then the necessary and sufficient condition for no diamond is $a_1 b b_1 < 0$.

Fact 3. Suppose the signs of a_1, b, b_1 and the magnitude of $|a_1|, |b|, |b_1|$ are fixed. Then the parameters satisfy $m_1 < m_2 + m_3$ produce more output spaces with positive topological entropies and higher ratio of diamonds than those satisfy $m_1 > m_2 + m_3$, where $m_1 > m_2 > m_3$ is the magnitude of $|a_1|, |b|, |b_1|$ in descending order.

For either Table 1(a) or (b) we can barely see diamonds in four specific rows, even though most parameters A, B, z in that partition make the output spaces with positive topological entropies. For example, consider the partition that A, B, z satisfy $b < a_1 < b_1 < 0$. There are total 52-subregions parameters that contribute positive topological entropies, and there is no diamond in any of them.

Consider the following cellular neural networks with input

$$\frac{dx_i}{dt} = -x_i + \sum_{k=0}^{n} a_{i+k} y_{i+k} + \sum_{k=0}^{n} b_{i+k} u_{i+k} + z, \quad k \in \mathbb{N}. \tag{9}$$

Denote by $\mathbf{Y_U}$ and $\mathbf{Y}$ the output and projection spaces, respectively. Below is our conjecture to generalize Facts 1 and 2.

Conjecture 1. Suppose a_k and b_k are nonzero for $k = 1, \ldots, n$.

(a) If $h(\mathbf{Y_U}) < h(\mathbf{Y})$, then $\min_{k>0}\{|b_k|\} > \max_{k>0}\{|a_k|\}$.
(b) If $\min_{k>0}\{|a_k|\} > \max_{k>0}\{|b_k|\}$, then

$$h(\mathbf{Y_U}) = h(\mathbf{Y}) \quad \Longleftrightarrow \quad \left(\prod a_k\right)\left(\prod b_k\right) < 0.$$

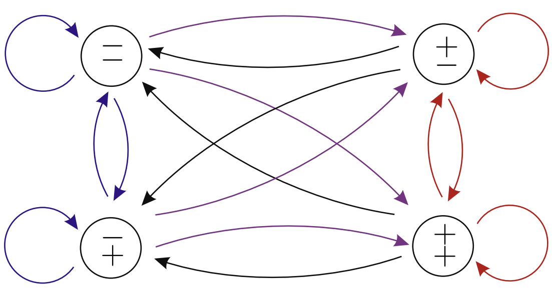

Fig. 3. Labeled graph representation of all admissible local output patterns for one-layer cellular neural networks with input. Those edges in the same color is labeled by the same symbol. Edges which are colored by blue, purple, black and red are labeled by – –, – +, + – and ++, respectively.

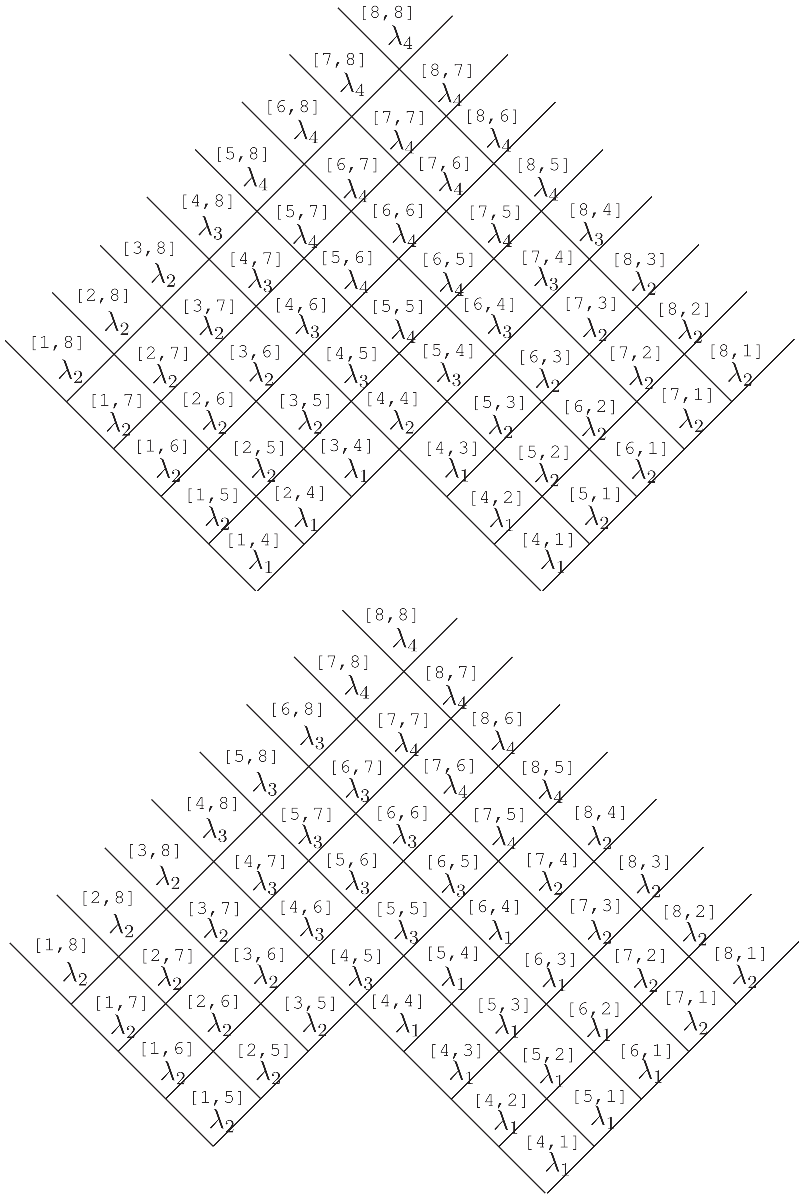

Fig. 4. The entropy diagram for one-layer cellular neural network satisfying b > −a1 > −b1 > 0 and b < −(a1 + b1). Those subregions with zero entropy are omitted and $\lambda_1 \approx \log 1.3247, \lambda_2 = \log g; \lambda_3 \approx \log 1.8393, \lambda_2 = \log 2$, where g is the golden mean.

Table 2
Diamonds that caused by different sets of local input from Fig. 4.

Input	Subregions with diamond	$h(\mathbf{Y_U})$
$--$	[7,4], [8,4], [4,5], [4,6], [4,7], [4,8]	$\log g$
$++$	[5,4], [6,4], [7,4], [8,4], [4,7], [4,8]	$\log g$
$--,++$	[5,4], [6,4], [7,4], [8,4], [4,5], [4,6], [4,7], [4,8]	$\log g$
$--,+-,++$	[5,4], [6,4], [7,4], [8,4], [4,5], [4,6], [4,7], [4,8]	$\log g$
$--,-+,++$	[5,4], [6,4], [7,4], [8,4], [4,5], [4,6], [4,7], [4,8]	$\log g$
$-+,+-$	[8,3], [4,8]	$\log 1.4142$
$--,-+,+-$	[5,3], [6,3], [4,4], [5,4], [6,4]	$\log 1.3247$
$--,-+,+-$	[7,4], [8,4]	$\log g$
$-+,+-,++$	[4,4], [3,5], [4,5], [3,6], [4,6]	$\log 1.3247$
$-+,+-,++$	[4,7], [4,8]	$\log g$

The dynamics of output space $\mathbf{Y_U}$ become more complicated when considering multi-layer cellular neural networks. Here we elucidating the following two-layer cellular neural network

$$\frac{dx_i^{(2)}}{dt} = -x_i^{(2)} + a^{(2)}y_i^{(2)} + a_1^{(2)}y_{i+1}^{(2)} + b^{(2)}u_i^{(2)} + b_1^{(2)}u_{i+1}^{(2)} + z^{(2)}, \tag{10}$$

$$\frac{dx_i^{(1)}}{dt} = -x_i^{(1)} + a^{(1)}y_i^{(1)} + a_1^{(1)}y_{i+1}^{(1)} + z^{(1)}, \tag{11}$$

where $u_i^{(2)} = y_i^{(1)}$ for $i \in \mathbb{Z}$. Suppose the parameters $a^{(k)}, a_1^{(k)}, z^{(k)}$ and $b^{(k)}, b_1^{(k)}$ are given for $k = 1, 2$, where $b^{(1)} = b_1^{(1)} = 0$. Let $\mathcal{B}^{(1)}$ and $\mathcal{B}^{(2)}$ be the set of admissible local patterns induced from (11) and (10), respectively. Without ambiguity we still denote the output space by $\mathbf{Y_U}$.

$$\mathbf{Y_U} = \{(y_j)_{j\in\mathbb{Z}} : \exists\ b_jb_{j+1} \in \mathcal{B}^{(1)} \text{such that} y_jy_{j+1} \diamondsuit b_jb_{j+1} \in \mathcal{B}^{(2)} \forall j \in \mathbb{Z}\}.$$

Question 2. Under which partition of the parameter space can we see the diamond? Is $\mathcal{B}^{(1)}$ and $\mathcal{B}^{(2)}$ related whenever there is diamond?

Suppose the parameters of (10) satisfy

$$b^{(2)} > -a_1^{(2)} > -b_1^{(2)} > 0, \quad b^{(2)} < -(a_1^{(2)} + b_1^{(2)}).$$

Fig. 4 are topological entropy diagrams which lists all subregions with positive topological entropies. The below diagram is obtained from the above diagram by assigning input patterns $\{--, -+, +-\}$. We notice that the diagram with assigned input patterns no longer maintain above diagram's symmetrical structure. Moreover, the topological entropies changes on some subregions. With appropriate choice of parameters in (11) we have the output local patterns of first layer (i.e., the assigned input local patterns) is $\{--, -+, +-\}$. One can see that the output space $\mathbf{Y_U}$ is capable of 4 different topological entropies either larger or less than the topological entropy $\log g$ of input space (the space generated by local input patterns).

Table 1 shows that, in Fig. 4, there are total 23-subregions inducing diamonds. Table 2 lists all subregions in these 23-subregions that caused diamonds again by different sets of local input. It is remarkable that only the last three sets of input patterns induce shift spaces with positive topological entropies themselves. Note that the first 5 sets of input patterns can only be induced when $a_1^{(1)} > 0$ while the last 5 sets can only be induced when $a_1^{(1)} < 0$.

Fact 4. $\{h(\mathbf{Y_U}) : a_1^{(1)} < 0\} \supset \{h(\mathbf{Y_U}) : a_1^{(1)} > 0\}$.

Proposition 2.1 indicates that $a_1^{(1)} < 0$ implies rich dynamics of the system. Fact 4 shows complicated input patterns induce rich phenomena for the output space.

In general, for two-layer cellular neural networks

$$\begin{aligned} \tfrac{dx_i^{(2)}}{dt} &= -x_i^{(2)} + \sum_{k=0}^{n} a_k^{(2)}y_{i+k}^{(2)} + \sum_{k=0}^{n} b_k^{(2)}u_{i+k}^{(2)} + z^{(2)}, \\ \tfrac{dx_i^{(1)}}{dt} &= -x_i^{(1)} + \sum_{k=0}^{n} a_k^{(1)}y_{i+k}^{(1)} + z^{(1)}, \end{aligned} \tag{12}$$

where $u_i^{(2)} = y_i^{(1)}$ for $i \in \mathbb{Z}$. Let $\mathbf{B}$ be the collection of sets of admissible local input of (12) except trivial input, that is, $\mathbf{B}$ consists of sets of admissible local patterns induced by one-layer cellular neural networks without input and $\{-,+\}^{\mathbb{Z}_{(n+1)\times 1}} \notin \mathbf{B}$. Write $\mathbf{B} = \cup_k \mathbf{B}_k$, where $\mathbf{B}_k$ is the collection of sets of admissible local patterns with $\#\{a_j^{(1)} : a_j^{(1)} < 0, j > 0\} = k$. Note that $\mathbf{B}_k \cap \mathbf{B}_\ell$ may not be empty. Denote by $\mathbf{Y_U}(\mathcal{B}^{(1)})$ the output space of (12) with admissible input patterns $\mathcal{B}^{(1)} \in \mathbf{B}$. We conjecture that

Conjecture 2. If $k > \ell$, then

$$\{h(\mathbf{Y_U}(\mathcal{B}^{(1)})) : \mathcal{B}^{(1)} \in \mathbf{B}_k\} \supset \{h(\mathbf{Y_U}(\mathcal{B}^{(1)})) : \mathcal{B}^{(1)} \in \mathbf{B}_\ell\}.$$

4. Proof of Theorems

Proof of Proposition 2.1. Suppose that $a_1 > 0$. Since the set of admissible local patterns $\mathcal{B}$ of output space $\mathbf{X}$ is a subset of $\{-,+\}^{\mathbb{Z}_{2\times1}}$, $\mathbf{X}$ is a one-step subshift of finite type. That is, there exists a graph representation $\mathcal{G}$ such that $\mathcal{G}$ completely realizes the dynamics of $\mathbf{X}$. Let $\mathcal{V}$ and $\mathcal{E}$ be the set of vertices and edges of $\mathcal{G}$, respectively. Then $\mathcal{V} = \{-,+\}$ and $|\mathcal{E}| = m + n \leqslant 4$, here m and n stands for the number of edges starting from $+$ and $-$, respectively.

Since the set of admissible local patterns is determined by

$$a - z - 1 > a_1y_{i+1} \quad \text{and} \quad a + z - 1 > -a_1y_{i+1},$$

every admissible local pattern has its priority once $y_i \in \{1, -1\}$ and a_1 are fixed. $a_1 > 0$ means that if $\mathbf{X}$ is not full shift then either the edge from $+$ to $-$ or the edge from $-$ to $+$ is not in $\mathcal{E}$. This implies the transition matrix $\mathbf{T}$ of $\mathcal{G}$ satisfies

$$\mathbf{T} \leqslant \begin{pmatrix} 1 & 1 \\ 0 & 1 \end{pmatrix} \quad \text{or} \quad \mathbf{T} \leqslant \begin{pmatrix} 1 & 0 \\ 1 & 1 \end{pmatrix}. \tag{13}$$

Hence $m+n \leqslant 3$ if and only if (13) holds. In other words, $m+n \leqslant 3$ if and only if $h(\mathbf{X}) = 0$.

If $a_1 < 0$, analogous argument indicates $m+n \geqslant 3$ if and only if

$$\mathbf{T} \geqslant \begin{pmatrix} 1 & 1 \\ 1 & 0 \end{pmatrix} \quad \text{or} \quad \mathbf{T} \geqslant \begin{pmatrix} 0 & 1 \\ 1 & 1 \end{pmatrix}.$$

For either case, the spectral radius of $\mathbf{T}$ is greater than or equal to golden mean. It is easily seen that replacing any nonzero element by 0 in either matrix makes spectral radius be less than or equal to 1. Therefore, $h(\mathbf{X}) > 0$ if and only if $m+n \geqslant 3$.

The proof is complete. $\square$

Proof of Proposition 2.2. Let $\mathcal{G}_{[m,n]} = (\mathcal{V}_{[m,n]}, \mathcal{E}_{[m,n]})$ and $\mathcal{G}_{[n,m]} = (\mathcal{V}_{[n,m]}, \mathcal{E}_{[n,m]})$ be the graph representation of $\mathbf{X}_{\mathcal{B}([m,n])}$ and $\mathbf{X}_{\mathcal{B}([n,m])}$, respectively. The proof of Proposition 2.1 shows that m and n are the numbers of edges starting from $+$ to $-$ and from $-$ to $+$, respectively. Note that herein

$$\mathcal{V}_{[m,n]}, \mathcal{V}_{[n,m]} \subseteq \left\{ \begin{matrix} - \\ - \end{matrix}, \begin{matrix} - \\ + \end{matrix}, \begin{matrix} + \\ - \end{matrix}, \begin{matrix} + \\ + \end{matrix} \right\} \equiv \{v_1, v_2, v_3, v_4\}.$$

See Fig. 3. Define $\Phi : \mathcal{G}_{\mathcal{B}([m,n])} \to \mathcal{G}_{\mathcal{B}([n,m)}$ by

$$\Phi(v_i) = v_{5-i}, \quad \Phi((v_i, v_j)) = (v_{5-i}, v_{5-j}).$$

It is easily seen that

(1) $v_i \in \mathcal{V}_{[m,n]}$ implies $v_{5-i} \in \mathcal{V}_{[n,m]}$, and
(2) $(v_i, v_j) \in \mathcal{E}_{[m,n]}$ implies $(v_{5-i}, v_{5-j}) \in \mathcal{E}_{[n,m]}$.

Thus Φ is well-defined and is a graph isomorphism. The isomorphism of $\mathcal{G}_{[m,n]}$ and $\mathcal{G}_{[n,m]}$ implements $\mathbf{X}_{\mathcal{B}([m,n])}$ is topological conjugate to $\mathbf{X}_{\mathcal{B}([n,m])}$. This completes the proof. $\square$

Before proving Theorem 3.1, we define a partial order for symbolic matrix. Let $\mathcal{A}$ be a finite set of alphabet containing empty symbol $\varnothing$ and let $\mathbf{A} = (\mathcal{A}, +)$ be an abelian additive group with identity element $\varnothing$. For $M, N \in \mathcal{M}_n(\mathbf{A})$, we define $M \geqslant N$ if and only if there exists $s_{ij} \in \mathbf{A}$ such that $m_{ij} = n_{ij} + s_{ij}$ for $1 \leqslant i,j \leqslant n$. Moreover, $M > N$ if $M \geqslant N$ and $M \neq N$.

Example 4.1. Suppose $\mathcal{A} = \{\varnothing, p, q\}$. Then $\mathbf{A}$ consists of elements of the form $np + mq$ for $n, m \in \mathbb{Z}$, and $\varnothing + \alpha = \alpha + \varnothing = \alpha$ for $\alpha \in \mathbf{A}$.

Suppose $M, N \in \mathcal{M}_2(\mathbf{A})$ such that

$$M = \begin{pmatrix} p & p \\ q & \varnothing \end{pmatrix}, \quad N = \begin{pmatrix} p & \varnothing \\ q & \varnothing \end{pmatrix}.$$

Then $M > N$ and $M + N = \begin{pmatrix} 2p & p \\ 2q & \varnothing \end{pmatrix}$.

Proof of Theorem 3.1. For simplicity, we only give the proof when b and b_1 are positive and the projection space $\mathbf{Y}$ is a full shift. $\#\mathcal{I}(y_0 y_1) \geqslant 2$ for each $y_0 y_1 \in \widetilde{\mathcal{B}}(A, B, z)$ asserts the symbolic transition matrix $\mathbf{T}$ for the labeled graph representation of $\mathbf{Y_U}$ satisfies

$$\mathbf{T} \geqslant \begin{pmatrix} s_1 & s_1 & s_2 & s_2 \\ \varnothing & \varnothing & \varnothing & \varnothing \\ \varnothing & \varnothing & \varnothing & \varnothing \\ s_3 & s_3 & s_4 & s_4 \end{pmatrix} \equiv \mathbf{H}.$$

The symbolic transition matrices $\widetilde{\mathbf{T}}$ and $\widetilde{\mathbf{H}}$, obtained by applying subset construction on $\mathbf{T}$ and $\mathbf{H}$ respectively, satisfy

$$\widetilde{\mathbf{T}} \geqslant \widetilde{\mathbf{H}} = \begin{pmatrix} \varnothing & \varnothing & \varnothing & \varnothing & s_1 & s_2 \\ \varnothing & \varnothing & \varnothing & \varnothing & \varnothing & \varnothing \\ \varnothing & \varnothing & \varnothing & \varnothing & \varnothing & \varnothing \\ \varnothing & \varnothing & \varnothing & \varnothing & s_3 & s_4 \\ \varnothing & \varnothing & \varnothing & \varnothing & s_1 & s_2 \\ \varnothing & \varnothing & \varnothing & \varnothing & s_3 & s_4 \end{pmatrix}.$$

Since the incidence matrix of $\widetilde{\mathbf{H}}$ has spectral radius $\rho = 2, h(\mathbf{Y_U}) \geqslant \log \rho = \log 2$. Moreover,

$$h(\mathbf{Y}) = \log 2 \geqslant h(\mathbf{Y_U}) \geqslant \log 2.$$

This completes the proof. $\square$

Proof of Theorem 3.3. Without loss of generality, we may assume that G is irreducible. Since G is essential, ϕ has a diamond indicates that there are two paths ω, τ in G with the same initial and terminate vertices such that $\mathcal{L}(\omega) = \mathcal{L}(\tau)$. The irreducibility of G asserts a path υ in G with $i(\upsilon) = t(\omega)$ and $t(\upsilon) = i(\omega)$. Moreover, $\omega\upsilon, \tau\upsilon$ are two loops in G implies $\mathbf{T}^{|\omega\upsilon|}(1 + i(\omega), 1 + i(\omega)) \geqslant 2$. This completes the proof. $\square$

5. Conclusion and discussion

In this paper we investigate and give necessary and sufficient conditions whether a two-layer cellular neural network has a diamond, respectively. Throughout the elucidation we focus on the case that each cell is only coupled with its righthand cell and the output patterns of the first layer are taken as input of the second layer. We have the following results.

(a) For one-layer cellular neural networks (4). Suppose a_1, b, b_1 are fixed. The symmetry of the entropy diagram in (a, z)-plane comes from the topological conjugacy of two systems. The asymmetry of two-layer cases indicates that the topological conjugacy no longer holds (cf. Fig. 4). In other words, the structure of the output spaces for one- and two- layer cellular neural networks are essentially different.
(b) A system has a diamond means the loss of information during the transfer. A necessary condition for diamond (D) is given and is checkable. We also demonstrate a checkable sufficient condition for the existence of diamond (Theorem 3.3).
(c) If the coefficients a_1, b_1 in (4) satisfies $b_1 > a_1$, then the system is likely to have a diamond.
(d) A two-layer cellular neural network (10) and (11) with $a_1^{(1)} < 0$ exhibits richer phenomena than $a_1^{(1)} > 0$ does. This is because the first layer is capable of more sets of output patterns when $a_1^{(1)} < 0$.

We propose two conjectures for cellular neural networks (9), (12) that each cell is only coupled with its right-hand side cells. Above results remain true if we consider (1) with $d = 1$ and $a_{-1}, b_{-1} \neq 0$. The case that $a_{-1}, b_{-1} \neq 0$ increases the complexity of partition of parameter space. Hence we only illustrate (4), (11) and (10) to clarify our argument.

Acknowledgement

The authors are grateful for the anonymous referees' valuable comments that improve the discussion of the elucidation. Ban is partially supported by the National Science Council, ROC (Contract No. NSC 102-2628-M-259-001-MY3) and National Center for Theoretical Sciences. Chang is partially supported by the National Science Council, ROC (Contract No. NSC 102-2115-M-035-004-).

References

[1] J.-C. Ban, C.-H. Chang, On the monotonicity of entropy for multi-layer cellular neural networks, Int. J. Bifur. Chaos Appl. Sci. Eng. 19 (2009) 3657–3670.
[2] J.-C. Ban, C.-H. Chang, Layer effect on multi-layer cellular neural networks, Appl. Math. Lett. 26 (2013) 706–709.
[3] J.-C. Ban, C.-H. Chang, S.-S. Lin, The structure of multi-layer cellular neural networks, J. Differ. Equ. 252 (2012) 4563–4597.
[4] J.-C. Ban, C.-H. Chang, S.-S. Lin, Y. -H Lin, Spatial complexity in multi-layer cellular neural networks, J. Differ. Equ. 246 (2009) 552–580.
[5] J.-C. Ban, S.-S. Lin, Patterns generation and transition matrices in multi-dimensional lattice models, Discrete Contin. Dyn. Syst. 13 (2005) 637–658.
[6] Mike Boyle, Karl Petersen, Hidden Markov processes in the context of symbolic dynamics, Entropy of Hidden Markov Processes and Connections to Dynamical Systems, Cambridge University Press, 2011. pp. 5–71.
[7] L.O. Chua, T. Roska, Cellular Neural Networks and Visual Computing, Cambridge University Press, 2002.
[8] K.R. Crounse, T. Roska, L.O. Chua, Image halftoning with cellular neural networks, IEEE Trans. Circuits Syst. 40 (1993) 267–283.
[9] R. Dogaru, L.O. Chua, Universal CNN cells, Int. J. Bifur. Chaos Appl. Sci. Eng. 9 (1999) 1–48.
[10] C.-H. Hsu, J. Juang, S.-S. Lin, W.-W. Lin, Cellular neural networks: local patterns for general template, Int. J. Bifur. Chaos Appl. Sci. Eng. 10 (2000) 1645–1659.
[11] J. Juang, S.-S. Lin, Cellular neural networks: mosaic pattern and spatial chaos, SIAM J. Appl. Math. 60 (2000) 891–915.
[12] B. Kitchens, Symbolic Dynamics. One-sided, Two-sided and Countable State Markov Shifts, Springer-Verlag, New York, 1998.
[13] J. Lam, S. Xu, Daniel W.C. Ho, Y. Zou, On global asymptotic stability for a class of delayed neural networks, Int. J. Circuit Theory Appl. 40 (2012) 1165–1174.
[14] M. Li, C.K. Tse, X. Ma, Calculation of steady-state solution of parallel-connected buck converters with active current sharing and its parameter sensitivity, Int. J. Circuit Theory Appl. 39 (2011) 275–297.
[15] S.-S. Lin, C.-W. Shih, Complete stability for standard cellular neural networks, Int. J. Bifur. Chaos Appl. Sci. Eng. 9 (1999) 909–918.
[16] D. Lind, B. Marcus, An Introduction to Symbolic Dynamics and Coding, Cambridge University Press, Cambridge, 1995.
[17] I. Petras, T. Roska, L.O. Chua, New spatial-temporal patterns and the first programmable on-chip bifurcation test bed, IEEE Trans. Circuits Syst. I, Fundam. Theory Appl. 50 (2003) 619–633.
[18] T. Roska, L.O. Chua, The cnn universal machine: an analogic array computer, IEEE Trans. Circuits Syst. II, Analog Digit. Signal Process. 40 (1993) 163–173.

[19] M. Storace, T. Poggi, Digital architectures realizing piecewise-linear multivariate functions: two FPGA implementations, Int. J. Circuit Theory Appl. 39 (2011) 1–15.
[20] Yuki Yayama, Existence of a measurable saturated compensation function between subshifts and its applications, Ergodic Theory Dynam. Syst. 31 (2011) 1563–1589.
[21] S.-N. Yu, C.-N. Lin, An efficient paradigm for wavelet-based image processing using cellular neural networks, Int. J. Circuit Theory Appl. 38 (2010) 527–542.